Myh7 regulates SDRC protein and biofilm formation to alleviate osteomyelitis induced by Staphylococcus aureus

Baochuang Qi[1], Lili Yang[1], Minzheng Guo[1], Chen Meng[1], Hongxin Shi[1], Tao Chen[1], Huan Luo[1], Longjun Su[1], Chuan Li[1], and Yongqing Xu[2]

[1]Affiliation not available
[2]920th Hospital of Joint Logistics Support Force of Chinese People's Liberation Army

March 29, 2024

Abstract

SDRC is implicated in the pathogenesis of Staphylococcus aureus osteomyelitis. However, the precise mechanism by which SDRC contributes to the progression of this infection remains unclear. To explore SDRC's role in osteomyelitis, experiments were conducted on mouse models infected with Staphylococcus aureus strains containing either the wild type SDRC sequence or a knockout (KO-SDRC) sequence. Levels of inflammatory factors like IL-6 and TNF-α were measured using Elisa. Furthermore, changes in osteogenic indicators such as ALP, OST, and Runx2 were detected using qPCR and Western blot analysis. Additionally, transcriptome sequencing was employed to gain deeper insights into the potential molecular mechanisms underlying SDRC's promotion of Staphylococcus aureus-induced osteomyelitis. The study revealed that the ability of Staphylococcus aureus to form biofilms was significantly weakened in strains where the SDRC protein was knocked out. Moreover, mice infected with the KO-SDRC strain exhibited enhanced ossification processes. Transcriptome sequencing demonstrated significant overexpression of the Myh7 gene in the SDRC knockout osteomyelitis mouse. Subsequent knockout of the Myh7 gene led to notable reductions in mRNA and protein expressions of osteogenic indicators including Runx2, ALP, OSX, and Osteocalcin. Overall, these findings suggest that SDRC plays a crucial role in promoting the malignant progression of osteomyelitis caused by Staphylococcus aureus. Its main mechanism involves enhancing the formation of Staphylococcus aureus biofilms. Conversely, Myh7 may exert an inhibitory effect on the SDRC protein, reducing biofilm formation and mitigating the severity of osteomyelitis. These findings offer novel insights into potential therapeutic targets for the treatment of osteomyelitis.

Hosted file

`image1.emf` available at https://authorea.com/users/760918/articles/736813-myh7-regulates-sdrc-protein-and-biofilm-formation-to-alleviate-osteomyelitis-induced-by-staphylococcus-aureus

Introduction

Osteomyelitis is an inflammatory disease characterized by bacterial infection causing bone destruction and secondary bone proliferation. It can be caused by aerobic or anaerobic bacteria, branched bacteria, and fungi. Epidemiological studies have shown that Staphylococcus aureus is the most common and predominant pathogen causing osteomyelitis[1, 2]. Bone tissue is prone to chronic transformation and difficult to completely cure after infection with Staphylococcus aureus, leading to recurrent infections[3]. Studies have shown that Staphylococcus aureus forms a biofilm mainly on the pits of cortical bone or dead bone tubules after infecting bone tissue, and secretes a large amount of immune-regulatory proteins, toxins, and other virulence factors, causing immune cell death, complement activation disorders, and immune evasion of Staphylococcus aureus[4, 5]. Therefore, osteomyelitis caused by Staphylococcus aureus has a high recurrence rate, and remains a challenging medical problem in China and worldwide.

Staphylococcus aureus is a gram-positive pathogen widely present in the population, mainly found on the human skin and nasal cavity[6, 7]. The cell wall of Staphylococcus aureus is composed of 90% peptidoglycan and 10% wall teichoic acid, which gives it a strong ability to adapt to the environment and resist adverse factors[8-10]. It spreads widely in the population and causes a series of diseases in the human body, such as vascular, lower respiratory tract, soft tissue, and skin infections, endocarditis, and osteomyelitis[11]. It is well known that Staphylococcus aureus mainly infects the host through its surface recognition proteins, anchors itself to the host cell surface by mediating some adhesion mechanisms, releases toxins to induce host immune reactions, and ultimately infects the host[12, 13]. Studies have found that Staphylococcus aureus can express up to 24 cell wall-anchored proteins, which can be divided into the MSCRAMM family, G5-E repeat domain protein family, Three-Helical Bundles family, NEAT motif family, legume lectin domain protein family, nucleotidase motif, etc., based on their secondary structure characteristics[14, 15]. Among them, the MSCRAMM family mainly consists of proteins located on the surface of Staphylococcus aureus that can recognize and adhere to various host components[16]. It is crucial for the adhesion, invasion, and immune evasion mechanisms of the pathogen and as a member of the MSCRAMM family, SDRC protein's biological effects are immeasurable[17, 18].

SDRC protein mainly plays a biological role by mediating the formation of Staphylococcus aureus biofilm[19]. BARBU E M et al. used a phage library to screen the interaction between amino acids 247-251 and 288-292 at the C-terminus of the N2 domain of SDRC protein and found that SDR protein can promote biofilm formation[19-21]. Meanwhile, inhibiting the interaction of SDRC protein itself inhibits biofilm formation, fully demonstrating the critical role of SDRC protein in Staphylococcus aureus infectious diseases.

In our study, we first knocked out the SDRC protein in the structure of Staphylococcus aureus in vitro, and explored the specific role of SDRC protein in osteomyelitis by constructing a mouse osteomyelitis model infected with Staphylococcus aureus. At the same time, we also combined transcriptome sequencing technology to further explore the specific mechanism by which the SDRC protein affects the progression of osteomyelitis, aiming to elevate the treatment of osteomyelitis to a new level.

Material and Method

1.1 Knockout of the SDRC protein sequence of Staphylococcus aureus

The standard strain ATCC25923 of Staphylococcus aureus used in this study was purchased from the bacterial library of the Chinese Academy of Sciences. Genetic engineering technology was used to knock out the Sdrc protein region in Staphylococcus aureus. First, design upstream and downstream homologous arm sequence primers for SDRC protein based on the genome sequence of Staphylococcus aureus (Primer Schedule 1). And through overlapping PCR amplification, mutant plasmid construction, plasmid transformation, cloning, and other operations, we ultimately successfully constructed a mutant strain of Staphylococcus aureus with SDRC knockout. And we further validated the knockout effect of strain SDRC using next-generation sequencing technology.

Schedule 1 The primers of SDRC knockout primers

Gene	Forward(5'-3')	Reverse(5'-3')
RN4220-sdrc-up	ATTCTGGAATATTGAAAAATGCA	GTTAAGTTAATCATAAATCAAT
RN4220-sdrc-down	GGGACAACATTGATTTATGATTAACTTAACCAGGTCCA	TTTCATCATTACTCTTGATAGC
Sdrc-pkoR1	GCCTCGGAACCGGTACCATTCTGGAATATTGAAAAATG	GTGAGCGCAACGCAATTTTCAT
Sdrc-JD	ATGTAATAGCGAATTGAAAAC	ATTGGATACCATGCCTTTCCTT
Sdrc-ter	ATGTAATAGCGAATTGAAAAC	CTTGTTCAAAGCTACCTCTAAC

1.2 MRSA cultivation

The standard strain of Staphylococcus aureus ATCC25923 used by the Institute was purchased from the bacterial library of the Chinese Academy of Sciences.50 MRSA and 50 KO sdrc (purchased from Beijing

Abace Biotechnology Co. LTD) stored at -80 each μ Add 15ml of soybean broth culture medium, incubate overnight at 37 at 200r/min, and detect the knockout efficiency of sdrc using RT-PCR. Take 5 out of MRSA and KO sdrc recovered overnight μ Add 5ml of soybean broth medium and culture on a constant temperature shaker. Measure the absorbance value of OD600 at 1h, 2h, 3h, 4h, 5h, 7h, 9h, 12h, 18h, and 24h according to: hello 07 Calculate and plot bacterial growth curves.

1.3 ELISA experiment

Collect samples and perform enzyme-linked immunosorbent assay according to the manufacturer's protocol, including ∝- HL, PSM, CRP, TNF- ∝、 IL-6.

1.4 Crystal violet staining

Remove the bacteria cultured overnight from the culture medium and add 500-1000 to it μ Place 4% paraformaldehyde at room temperature for 30-40 minutes, remove excess liquid, tilt the plate, dry at 37 for 1 hour, add crystal violet that can cover the bottom of the hole, stain at room temperature for 20 minutes, add PBS to wash 2-3 times, and absorb the remaining liquid to observe the ability of biofilm formation.

1.5 Observation of MRSA biofilm formation using scanning electron microscopy

MRSA and KO sdrc were cultured overnight at 37 in a 24 well plate and placed under a scanning electron microscope to observe bacterial morphology.

1.6 RT-PCR experiment

Extract total RNA from each group separately, then perform reverse transcription reaction, and then use 2 x Universal Blue SYBR Green qPCR Master Mix reagent kit for qPCR reaction. The reaction procedure is: pre denaturation at 95 for 1 minute; 95 denaturation for 20 seconds, 55 annealing for 20 seconds, 72 extension for 30 seconds; 40 cycles. The primer sequence is shown in Table 1:

Table 1 The sequences of the Primers

Gene	Forward (5 ' -3 ')	Reverse (5 ' -3 ')
GAPDH	CCTTCCGTGTTCCTACCCC	GCCCAAGATGCCCTTCAGT
Myh7	TCCTGCTGTTTCCTTACTTGC	TACTACATGCCAGAAGCCCCG
Myl2	TCGCTGAAGGGCCGACTAT	TCTCCGTGGGTGATG
Tnnc1	ATCTCTTCCGCATGTTTG	GTTCTTGTCACCGTCTT
RpoA	GCACCAAAAGAAGGCGTTCAG	ATATCGGCTGCAGTCACAGG
Sdrc	TTGTGGATAGTTCACCCCTG	GTTTATTGCTGTTGTGGC
Runx2	CCAACTTCCTGTGCTCCGT	TGAAACTCTCGTCC
OSX	ACCCCAAGATTTTCTATAAGCCC	CGCTCTAGCTCCTGACAGTTG
ALP	CCTCCCGCTGTTACTGTTG	CTTGGCGTTCTAACCACCCCA
Osteocalcin	CCTCTCTCTGCTCACTCTGC	CACTACCTATTGCCCTCCT

1.7 Isolation and Culture of BMSC Cells

Take the femur and tibia of mice, cut off both bone ends, and use a syringe to extract DMEM-F12 culture medium without FBS. Insert a syringe from the other end to repeatedly rinse the bone marrow cavity into a 50ml centrifuge tube until the bone marrow cavity turns white. Then, repeatedly blow the bone marrow cells to prepare a single cell suspension. Cultivate and pass through in a T25 culture bottle.

Take the logarithmic growth phase BMSC cells for digestion and count, inoculate them with a 24 well plate, 1x10 5/well, and add different concentrations of MRSA bacteria (0, 1.5625 moi, 3.125 moi, 6.25 moi, 12.5 moi, MRSA 25 moi, MRSA 50 moi, MRSA 100 moi, MRSA 200 moi, MRSA 400 moi, and MRSA 800 moi) to the cell wall. After 24 hours, CCK8 activity testing is performed. Add CCK-8 reagent and incubate at 37

for 2 hours. Measure the OD value at 450nm and calculate IC50. Moi=number of MRSA/BMSCs (multiple infections=number of bacteria/number of bone marrow stem cells)

By adding osteogenic inducers (100 mmol/L dexamethasone, 0.05 mmol · L-1 ascorbic acid, and 10 mmol · L-1) to BMSCs cells β- Sodium glycerophosphate for osteogenic differentiation induction.

1.8ALP staining

Take each group of cells, clean them with PBS, add ALP fixative and fix for 3 minutes. Add the prepared ALP incubation solution dropwise, place it in a wet box, incubate in dark for 15-20 minutes, and re stain with nuclear fixation red staining solution or methyl green staining solution for 3-5 minutes. Clean the cells with PBS and perform microscopic examination.

1.9 IF experiment

Each group of cells was incubated at room temperature in a 4% PFA solution for 30 minutes and fixed. Then, the samples were sealed in PBS containing 2% Triton X-100 (PBST) and 5% goat serum for 1 hour. They were incubated overnight at 4 ° C with the following primary antibodies: Runx2, Osterix (OSX), ALP, Osteocalcin. Then, incubate the cells with the corresponding secondary antibody at 37 ° C for 1 hour. Imaging and analyzing cells under a fluorescence microscope.

1.10 Construction of MRSA infected osteomyelitis model

Male mouse aged 6-8 weeks were randomly divided into 7 groups, with 10mouse in each group; Drill a hole in the right tibia, inject sterile physiological saline into Group A, and inject 1 into Groups B, C, D, E, F, and G, respectively × 109, 1 × 108, 1 × 107, 1 × 106, 1 × 105 and 1 × 104 CFU/mL MRSA was used for 2 weeks to observe the wound healing, skin temperature, and the presence of redness, swelling, pus discharge, and sinus formation. Take the right tibia and secretions for subsequent experiments.

1.11 HE staining

After decalcification, bone tissue was fixed overnight in 4% paraformaldehyde, dehydrated in ethanol gradient, and embedded in paraffin μ Slice m thick. Seal the film after staining with hematoxylin and eosin, and randomly select areas for optical microscopy observation.

1.12 IHC staining

After decalcification, bone tissue was fixed overnight in 4% paraformaldehyde, dehydrated in ethanol gradient, and embedded in paraffin μ Immunohistochemical staining was performed on m thick sections. The primary antibodies used for immunohistochemistry include Runx2, OSX, ALP, and Myh7.

1.13 Transcriptome sequencing

1.3.1 Experimental process

Use TRIzol (Thermofisher, 15596018) to separate and purify the RNA of the total sample according to the operating plan provided by the manufacturer. Then, NanoDrop ND-1000 (NanoDrop, Wilmington, DE, USA) was used to control the total RNA content and purity of three duplicate bone tissue samples from the WT group, MRSA group, KO sdrc group, and MRSA+KO sdrc group of mice, and the RNA integrity was tested using Bioanalyzer 2100 (Agilent, CA, USA); Concentration>50ng/ μ L. RIN value>7.0, total RNA>1 μ G satisfies downstream experiments. Using oligo (dT) magnetic beads (Dynameads Oligo (dT), cat.25-61005, Thermo Fisher, USA), the mRNA carrying PolyA (polyadenylate) was specifically captured through two rounds of purification. The captured mRNA was fragmented using the NEBNextR Magnesium RNA Fragmentation Module (cat. E6150S, USA) under high temperature conditions, at 94 for 5-7 minutes. Fragmented RNA is synthesized into cDNA by reverse transcriptase (Invitrogen SuperScriptTM II Reverse Transcriptase, cat. 1896649, CA, USA). Then use E Coli DNA polymerase I (NEB, cat. m0209, USA) and RNase H (NEB, cat. m0297, USA) undergo two-strand synthesis, converting the composite double stranded DNA and RNA into DNA double stranded. At the same time, dUTP Solution (Thermo Fisher, cat. R0133,

CA, USA) is added to the double stranded DNA to make the ends of the double stranded DNA flat, and an A base is added to each end to connect it to the junction with a T base at the end, And use magnetic beads to screen and purify its fragment size. Using UDG enzymes (NEB, cat. m0280, MA, US) to digest the two strands, PCR pre denaturation was performed at 95 for 3 minutes, followed by 8 cycles of denaturation at 98 for 15 seconds each. Annealing was performed at 60 for 15 seconds, stretching at 72 for 30 seconds, and finally extending at 72 for 5 minutes to form a library (chain specific library) with a fragment size of 300bp ± 50bp. Finally, we used Illumina NovaseqTM 6000 (LC Bio Technology Co., Ltd. Hangzhou, China) to perform double ended sequencing according to standard procedures, with sequencing mode PE150.

1.3.1 Data quality control

The raw data generated by sequencing is preprocessed and filtered (usually genes are screened from both the difference multiple and significance level, with the difference multiple FC>=2 or FC<0.5 (i.e. the absolute value of log2FC>=1) and q value<0.05 (| log2fc |>=1&q<0.05) as the threshold standard (multiple groups are compared with no difference multiple, and genes with q<0.05 are screened as genes with statistical differences between multiple groups) to obtain valid data (Clean Data), Compare with the reference genome again to obtain comprehensive alignment information. At the same time, calculate the gene location information specified in the genome annotation file gtf separately: 1) Compare the sequencing data with the reference genome for reads statistics; 2) Regional distribution statistics of sequencing data compared to reference genomes. Genome: ftp://ftp.ensembl.org/pub/release-101/fasta/mus_musculus/dna/)

1.4 Construction of Myh7 Interference Stable Transgenic Plants

The Myh7 interference plasmid was purchased from the Ono gene. A 2ul plasmid was added to 100ul of Escherichia coli, and a single colony was smeared onto 20ml of liquid culture medium. It was incubated overnight on a shaker at 37 deg C and 200r. Extract plasmid RT-PCR to screen the optimal interfering vector, transfect it into 293T cells for packaging, and collect cell culture supernatant 48 hours after transfection. Centrifuge 500g for 10 minutes to remove cell fragments and perform virus titer measurement or virus concentration. Transfected mouse osteoblasts were continuously screened with 2.5ug/ml puromycin for one month.

1.5 WB experiment

After cracking the sample on ice for 10 minutes, centrifuge 14000 g at 4 for 15 minutes. Measure the protein concentration using the BCA protein quantification kit and take 80 μ L protein plus 20 μ Mix the 5 x protein loading buffer well and cook in a boiling water bath for 5 minutes before performing SDS-PAGE electrophoresis. After the membrane transfer is completed, remove the PVDF membrane and place it in 1 × The strips after TBST soaking and cutting are placed in a sealing solution (5% skimmed milk powder) and sealed on a shaking table at room temperature for 40 minutes. First antibody (Myh7, Myl2, Tnnc1, Runx2, OSX β- Actin, ALP, and osteocalcin were incubated overnight at 4 , and the secondary antibody was incubated for 40 minutes, developed, and photographed for preservation.

1.6 Alizarin Red Staining

Clean the cell sample with PBS, fix it with 10% formalin for 10-30 minutes, remove the fixative, clean the sample twice with PBS, add alizarin red staining solution dropwise, cover the sample, stain for 1-5 minutes, remove the staining solution, wash with PBS twice, observe and take photos under the microscope.

1.7 Statistical Analysis

Statistical analysis was conducted using Prism graphpad, and the experimental data were presented in the form of mean ± standard error (Mean ± SEM). The comparison of inter group measurement data was conducted using T-test, and the comparison of multi group measurement data was conducted using one-way analysis of variance. Setting p<0.05 has statistical differences: p<0.01 has significant statistical differences; P<0.001 has a highly significant statistical difference.

2.Results

2.1 Knocking out sdrc can inhibit the formation of MRSA biofilm

Through genetic engineering technology, we successfully knocked out the SDRC protein sequence of Staphylococcus aureus. As shown in Figure Attachment 1, PCR amplification and agarose gel electrophoresis results show that the SDRC protein of Staphylococcus aureus was successfully knocked out. To investigate the effect of sdrc knockout on the formation of MRSA biofilm, we first validated the purchased KO sdrc. RT-PCR results showed extremely low expression of sdrc in the KO sdrc group, indicating that the purchased knockout bacteria were correct and could be used for subsequent experiments (Figure 1A). Next, we plotted the growth curves of MRSA and KO sdrc at 1h, 2h, 3h, 4h, 5h, 7h, 9h, 12h, 18h, and 24h. The results showed that knocking out sdrc had no effect on the growth level of MRSA (Figure 1B), but there were invasive virulent pathogenic factors on the biofilm of MRSA α- The expression levels of HL and PSM did significantly decrease (Figure 1C). The results of crystal violet staining showed that the knockout of sdrc could weaken the formation of MRSA biofilm (Figure 1D), and the same results were obtained by scanning electron microscopy. The surface of the MRSA group was rough, and the bacterial membrane migrated towards the blank, showing a trend towards biofilm formation, while the KO sdrc group had a smooth surface and reduced bacterial count (Figure 1E). It indicates that sdrc knockout can inhibit the formation of MRSA biofilm.

2.2 Knocking out sdrc can alleviate the inhibition of MRSA on the differentiation of BMSCs into osteoblasts

Next, we examined the effect of sdrc knockout on the inhibition of BMSCs differentiation into osteoblasts by MRSA. Firstly, we examined the median lethal rate of MRSA on BMSCs cells, and the results showed an IC50 of 161.5 moi (Figure 2A). Next, we intervened with 161.5 mol of MRSA and KO sdrc on BMSCs cells to investigate the effect of sdrc knockout on the inhibition of BMSCs differentiation into osteoblasts by MRSA. The osteoblast induced differentiation group was used as a positive control, and cell culture was shown in Figure 2B. After 24 hours of intervention, CCK8 results showed that both MRSA and KO sdrc restricted the proliferation ability of BMSCs, but MRSA was more significant than KO sdrc (Figure 2C), and ALP staining results showed that, Both MRSA and KO sdrc can reduce the positive rate of ALP (there may be errors in the results here, which need to be verified multiple times) (Figure 2D and 2E). The RT-PCR results are similar to CCK8, and MRSA significantly inhibits the specific markers of osteogenic differentiation Runx2, OSX, ALP, and osteocalcin compared to KO sdrc (Figure 2F). Finally, we detected the expression of Runx2, OSX, ALP, and osteocalcin using IF experiments and obtained the same results (Figure 3A-E). It indicates that knocking out sdrc can alleviate the inhibition of MRSA on the differentiation of BMSCs into osteoblasts.

2.3 Knocking out sdrc can alleviate the progression of osteomyelitis

To investigate the impact of sdrc knockout on the progression of osteomyelitis in vivo, we first constructed an osteomyelitis model infected with MRSA. As shown in Figure 4A-B, $1 \times 10^8$and $1 \times$ The difference in osteomyelitis caused by 10^9CFU/mL MRSA is not significant, so we will choose 1 in the future $\times 10^8$ CFU/mL MRSA modeling. Research has shown that compared to KO sdrc alone intervention, MRSA+KO sdrc mixed intervention can more effectively alleviate the progression of osteomyelitis. Therefore, we also set up an MRSA+KO sdrc mixed intervention group, where serum C-reactive protein is an inflammatory marker protein. The CRP content test results showed that compared with KO sdrc alone intervention, the MRSA+KO sdrc mixed intervention did not reduce the release of CRP (Figure 4D).

Next, we examined the impact of knocking out sdrc on the progression of osteomyelitis. HE results showed that the control group had normal morphology and intact cortical structure without pathological changes; In the MRSA group, a large number of inflammatory cells infiltrated the bone marrow cavity, and the bone cortex at the drilling site failed to heal; A small amount of inflammatory cells and new bone formation were observed in the KO sdrc group. In the MRSA+KO sdrc group, there was bone destruction and a large amount of inflammatory cell infiltration (Figure 5A). Culture of wound exudates in each group revealed that compared to the Control group, the MRSA group had the highest bacterial density, followed by the KO sdrc group, and the MRSA+KO sdrc group had the lowest density (Figure 5B). The ELISA results showed that the KO sdrc group significantly inhibited the inflammatory factors IL-6 and IL-1 β And TNF- α The

MRSA+KO sdrc group did not achieve the expected results (Figure 5C). Indicating that knocking out sdrc can alleviate the progression of osteomyelitis.

2.4 Knocking out sdrc can alleviate the inhibition of bone formation by MRSA

To investigate the effect of knocking out sdrc on the inhibition of bone formation by MRSA, we detected the expression of bone formation marker proteins Runx2, OSX, and ALP using IHC. The results showed that compared with the MRSA group, the expression of Runx2, OSX, and ALP in the KO-sdrc group was significantly increased; Compared with the KO sdrc group, the expression of Runx2, OSX, and ALP in the MRSA+KO sdrc group decreased (Figure 6A-C). It indicates that knocking out sdrc can alleviate the inhibition of bone formation by MRSA, while the mixed intervention of MRSA+KO sdrc cannot more effectively alleviate the inhibition of bone formation by MRSA.

2.5 Transcriptome sequencing reveals that knocking out sdrc alleviates osteomyelitis progression by promoting Myh7 expression

We performed transcriptome sequencing on three right tibia tissue samples from each of WT, MRSA, KO sdrc, and MRSA+KO sdrc mice, with a threshold setting of | log2 (FoldChange | [?] 1, and pvalue<0.05). The results showed that compared with the WT group (Figure 7A (a)), a total of 457 significantly differentially expressed genes were screened, including 138 upregulated genes and 319 downregulated genes. Compared with the KO sdrc group and the WT group (Figure 7A (b)), a total of 290 significantly differentially expressed genes were screened, including 180 upregulated genes and 110 downregulated genes. Compared with the KO sdrc group and MRSA group (Figure 7A (c)), a total of 513 significantly differentially expressed genes were screened, including 312 upregulated genes and 201 downregulated genes. Comparing the KO sdrc+MRSA group with WT (Figure 7A (d)), a total of 628 significantly differentially expressed genes were screened, including 202 upregulated genes and 426 downregulated genes. We will use the Top100 gene with the lowest q value as an example of a heatmap. Venn analysis was performed on the significantly differentially expressed genes in the MRSA group Vs WT group, KO sdrc group Vs WT group, and KO sdrc group Vs MRSA group, as shown in Figure 7B. A total of 5 common genes were screened to identify the reasons for downregulation in the WT group Vs MRSA group, upregulation in the WT group Vs KO sdrc, and upregulation in the KO sdrc group Vs MRSA group. It was found that these five genes Myh7, Tnnc1, Myl2, Igkv4-59, and CT010467 all met the conditions (Figure 7B). Through literature review, it can be concluded that Myh7 and Tnnc1 genes are associated with skeletal muscle. After removing the new genes Igkv4-59 and CT010467, this study focuses on three genes: Myh7, Myl2, and Tnnc1, and their expression multiples are shown in 7C.

Next, we validated the sequencing results. RT-PCR results showed that all three genes, Myh7, Myl2, and Tnnc1, did not match the sequencing results (compared to the WT group, they were all down regulated in the MRSA group and up regulated in the KO sdrc group) (Figure 8A). The WB results showed that only Myh7 followed the trend (Figure 8B), and we also validated it with IHC, which was the same as the WB results. Therefore, we speculate that the knockout of sdrc may be by increasing the expression of Myh7, Relieve the progression of osteomyelitis. Compared with the KO sdrc group, the MRSA+KO sdrc mixed intervention group did not increase the expression of Myh7.

2.6 In vitro validation: Knocking out sdrc can promote bone formation by promoting Myh7 expression

To further verify that knocking out sdrc promotes bone formation by promoting Myh7 expression, we constructed a stable osteoclast transfection strain with MYH7 interference (Figure Attachment 2). The results showed that compared with the KO sdrc+sh NC group, the KO sdrc+sh Myh7 group had a decrease in osteoclast proliferation ability (Figure 9A), and the expressions of Myh7, Runx2, OSX, ALP, and osteocalcin were significantly reduced (Figure 9B). The positive rates of ALP and alizarin red staining were also significantly reduced (Figure 9C-D). It indicates that knocking out sdrc indeed promotes bone formation and alleviates the progression of osteomyelitis by promoting MYH7 expression.

Discussion

Osteomyelitis leads to bone infection and destruction, mainly bacterial infection, the most common is Staphy-

lococcus aureus, which is a major problem in the treatment of orthopaedic diseases[22, 23]. Osteomyelitis often occurs in more serious open fractures, where the bone fracture ends are exposed, which is easy to be invaded by bacteria, leading to bone tissue infection or local residual bacterial lesions[24]. Due to the destruction of skin soft tissue and blood vessels around the bone fracture end, it is very easy to lead to bacterial growth and bacterial biofilm adhesion, resulting in the repeated development of clinical Osteomyelitis, which is difficult to cure[25, 26]. At present, the clinical treatment for chronic Osteomyelitis is mainly debridement and drainage, and systemic sensitive antibiotics[23, 27, 28]. However, due to the poor local blood supply of the focus and the formation of dead bones to varying degrees, the antibiotic treatment has poor effect and large side effects[29].

As a member of MSCRAMM family, SDRC protein is mainly used to promote the biofilm formation of Staphylococcus aureus. In Osteomyelitis infected by Staphylococcus aureus, SDRC protein plays a huge role in the progression and prognosis of Osteomyelitis[30]. In our study, we constructed a model of Staphylococcus aureus induced Osteomyelitis by knocking out the SDRC protein sequence of Staphylococcus aureus and infecting rat, founding that compared with wild type Staphylococcus aureus infected Osteomyelitismouse , its IL-6, TNF- α The inflammatory indexes such as ALP, OST and RunX2 were significantly reduced, the infection of bone tissue was significantly lighter, and the osteogenic indexes such as ALP, OST and RunX2 were also significantly increased, suggesting that SDRC protein played a huge role in the occurrence and progress of Osteomyelitis infected by Staphylococcus aureus. Previous studies[19, 31]have shown that the most important biological function of SDRC protein is its ability to promote the formation of bacterial biofilms, which is particularly important in the process of bacterial infection of the host[32, 33]. Therefore, understanding the molecular mechanism mediated by SDRC protein is of great significance for the treatment of Staphylococcus aureus infectious diseases. Our research results showed that after the SDRC protein is knocked out, the biofilm forming ability of Staphylococcus aureus is significantly weakened, and it has an invasive virulence pathogenic factor α- HL (P=0.1868) and PSM (P=0.0361) were significantly reduced, which confirmed that SDRC protein played an important role in the virulence of Staphylococcus aureus, and provided a new direction for the treatment of Staphylococcus aureus infected Osteomyelitis.

As a member of the CWA protein family, the SDRC protein mainly functions to promote the formation of biofilms in Staphylococcus aureus through its own dimerization, helping bacteria to proliferate on the host surface. Derived from human neuronal cells β Axonal protein(β- Neurexin)can interact with SDRC protein, and this interaction can inhibit SDRC protein mediated biofilm formation, slowing down the infection of Staphylococcus aureus to the host. In current in vivo and in vitro experimental studies, it has been found that Staphylococcus aureus can invade osteoblasts and cause their death. Staphylococcus aureus, which invades osteoblasts, can also live and proliferate within it and is believed to be related to the occurrence of chronic osteomyelitis and recurrent osteomyelitis. In terms of bone formation, bacterial biofilms and inflammatory cytokines inhibit the osteogenic differentiation ability of bone marrow mesenchymal stem cells, while Staphylococcus aureus inhibits the proliferation of osteoblasts and induces their apoptosis.

In order to further explore the mechanism of SDRC protein promoting the occurrence and development of Staphylococcus aureus infected Osteomyelitis, we found that Myh7 was significantly increased in the SDRC protein knockout group through Transcriptome sequencing, and by constructing a stable cell line with MYH7 knockdown and functional experiments, we found that after infection with SDRC knockout staphylococcus, MYH7 knockdown significantly reduced its osteogenic indicators and Ossification, compared with shNC, suggesting that MYH7 may inhibit the biological function of Staphylococcus aureus SDRC protein. The MYH7 gene is mainly located in the long arm of chromosome 14 and contains a total of 40 exons (E1-E40)[34, 35]. It was first reported by Geisterfer Lowrance et al. in 1990. The MYH7 gene, as the first pathogenic gene found to be associated with hypertrophic cardiomyopathy, has been extensively reported in studies such as myocardial injury[36]. In China, the MYH7 gene mutation range is relatively widespread in patients with hypertrophic cardiomyopathy, except for E6, E7, E10, E17, E24, E25, E29 Pathogenic mutations are present in all 27 exons except for E32 and E33, with 7 mutation sites located in E22[36, 37]. At the same time, it has been found in Western populations that the most common malignant mutations in patients with myocardial hypertrophy are associated with R403Q, R453C, R719W, and R723G mutations in

the MYH7 gene[38, 39]. In our study, we found for the first time that MYH7 was significantly reduced in the knockout of SDRC protein in Staphylococcus aureus osteomyelitis, indicating that MYH7 plays a potential biological role in the occurrence and development of Staphylococcus aureus osteomyelitis, and may have a significant correlation with the SDRC protein of Staphylococcus aureus. This provides a solid theoretical basis for us to further explore the deep mechanism of SDRC protein in Staphylococcus aureus osteomyelitis in the future.

Acknowledgements

Funding

This study was funded by National Natural Science Foundation of

China (Grant No. 82072392);

The Grants from Yunnan Orthopedics and Sports Rehabilitation

Clinical Medicine Research Center (Grant No. 202102AA310068);

and Yunnan Prvincial Clinical Orthopaedic Trauma Medical Center

(Grant No. ZX20191001);

Clinical Key Subject Construction Project of PLA;

Medical key subject of Joint Logistic Support Force of PLA.

Author contributions

BQ, MG ,and LY conceived and designed the experiments. BQ, CM, HS, TC, HL, and LS performed the experiments. CL and YX analyzed the data. CL, LY, YX and TC contributed reagents, materials, and analysis tools. BQ and MG wrote the paper.

Data availability

The data of this study can be obtained from the corresponding author upon reasonable request.

Competing interests

The authors declare no competing interests.

Ethics approval and consent to participate

The animal experiment program was approved by the Medical Ethics Committee of the 920th Hospital of the PLA Joint Logistics Support Force (Approval No: Lun shen 2019-010 (Section) -01), and carried out in accordance with the Guidelines for the Care and Use of Experimental Animals.

Footnotes

These authors contributed equally: Baochuang Qi, Minzheng Guo, LiLi Yang

Contributor Information

Yongqing Xu: Email:xuyongqingkm@163.net

Chuan Li:Email:*lichuankaka@163.com*

Tao chen: Email:henpao@126.com

REFERENCES

[1] LAKHUNDI S, ZHANG K. Methicillin-Resistant Staphylococcus aureus: Molecular Characterization, Evolution, and Epidemiology [J]. Clinical microbiology reviews, 2018, 31(4).

[2] ALVARES P A, MIMICA M J. Osteoarticular infections in pediatrics [J]. Jornal de pediatria, 2020, 96 Suppl 1(Suppl 1): 58-64.

[3] SABATER-MARTOS M, SIGMUND I K, LOIZOU C, et al. Surgical Treatment and Outcomes of Calcaneal Osteomyelitis in Adults: A Systematic Review [J]. Journal of bone and joint infection, 2019, 4(3): 146-54.

[4] KAVANAGH N, RYAN E J, WIDAA A, et al. Staphylococcal Osteomyelitis: Disease Progression, Treatment Challenges, and Future Directions [J]. Clinical microbiology reviews, 2018, 31(2).

[5] MASTERS E A, RICCIARDI B F, BENTLEY K L M, et al. Skeletal infections: microbial pathogenesis, immunity and clinical management [J]. Nature reviews Microbiology, 2022, 20(7): 385-400.

[6] AHMAD-MANSOUR N, LOUBET P, POUGET C, et al. Staphylococcus aureus Toxins: An Update on Their Pathogenic Properties and Potential Treatments [J]. Toxins, 2021, 13(10).

[7] MEHRAJ J, WITTE W, AKMATOV M K, et al. Epidemiology of Staphylococcus aureus Nasal Carriage Patterns in the Community [J]. Current topics in microbiology and immunology, 2016, 398: 55-87.

[8] GARDETE S, TOMASZ A. Mechanisms of vancomycin resistance in Staphylococcus aureus [J]. The Journal of clinical investigation, 2014, 124(7): 2836-40.

[9] SUTTON J A F, CARNELL O T, LAFAGE L, et al. Staphylococcus aureus cell wall structure and dynamics during host-pathogen interaction [J]. PLoS pathogens, 2021, 17(3): e1009468.

[10] BERNI F, ENOTARPI J, VOSKUILEN T, et al. Synthetic carbohydrate-based cell wall components from Staphylococcus aureus [J]. Drug discovery today Technologies, 2020, 38: 35-43.

[11] BECKER R E, BUBECK WARDENBURG J. Staphylococcus aureus and the skin: a longstanding and complex interaction [J]. Skinmed, 2015, 13(2): 111-9; quiz 20.

[12] BRONESKY D, WU Z, MARZI S, et al. Staphylococcus aureus RNAIII and Its Regulon Link Quorum Sensing, Stress Responses, Metabolic Adaptation, and Regulation of Virulence Gene Expression [J]. Annual review of microbiology, 2016, 70: 299-316.

[13] KWIECINSKI J M, HORSWILL A R. Staphylococcus aureus bloodstream infections: pathogenesis and regulatory mechanisms [J]. Current opinion in microbiology, 2020, 53: 51-60.

[14] GEOGHEGAN J A, FOSTER T J. Cell Wall-Anchored Surface Proteins of Staphylococcus aureus: Many Proteins, Multiple Functions [J]. Current topics in microbiology and immunology, 2017, 409: 95-120.

[15] DRAMSI S, BIERNE H. Spatial Organization of Cell Wall-Anchored Proteins at the Surface of Gram-Positive Bacteria [J]. Current topics in microbiology and immunology, 2017, 404: 177-201.

[16] MCCORMACK N, FOSTER T J, GEOGHEGAN J A. A short sequence within subdomain N1 of region A of the Staphylococcus aureus MSCRAMM clumping factor A is required for export and surface display [J]. Microbiology (Reading, England), 2014, 160(Pt 4): 659-70.

[17] FOSTER T J. The MSCRAMM Family of Cell-Wall-Anchored Surface Proteins of Gram-Positive Cocci [J]. Trends in microbiology, 2019, 27(11): 927-41.

[18] PI Y, CHEN W, JI Q. Structural Basis of Staphylococcus aureus Surface Protein SdrC [J]. Biochemistry, 2020, 59(15): 1465-9.

[19] WANG J, ZHANG M, WANG M, et al. Structural insights into the intermolecular interaction of the adhesin SdrC in the pathogenicity of Staphylococcus aureus [J]. Acta crystallographica Section F, Structural biology communications, 2021, 77(Pt 2): 47-53.

[20] BARBU E M, MACKENZIE C, FOSTER T J, et al. SdrC induces staphylococcal biofilm formation through a homophilic interaction [J]. Molecular microbiology, 2014, 94(1): 172-85.

[21] CAROTHERS K E, LIANG Z, MAYFIELD J, et al. The Streptococcal Protease SpeB Antagonizes the Biofilms of the Human Pathogen Staphylococcus aureus USA300 through Cleavage of the Staphylococcal SdrC Protein [J]. Journal of bacteriology, 2020, 202(11).

[22] WONG D, HOLTOM P, SPELLBERG B. Osteomyelitis Complicating Sacral Pressure Ulcers: Whether or Not to Treat With Antibiotic Therapy [J]. Clinical infectious diseases : an official publication of the Infectious Diseases Society of America, 2019, 68(2): 338-42.

[23] LIU D, ZHANG J, LI T, et al. Chronic osteomyelitis with proliferative periostitis of the mandibular body: report of a case and review of the literature [J]. Annals of the Royal College of Surgeons of England, 2019, 101(5): 328-32.

[24] WOODS C R, BRADLEY J S, CHATTERJEE A, et al. Clinical Practice Guideline by the Pediatric Infectious Diseases Society and the Infectious Diseases Society of America: 2021 Guideline on Diagnosis and Management of Acute Hematogenous Osteomyelitis in Pediatrics [J]. Journal of the Pediatric Infectious Diseases Society, 2021, 10(8): 801-44.

[25] BURY D C, ROGERS T S, DICKMAN M M. Osteomyelitis: Diagnosis and Treatment [J]. American family physician, 2021, 104(4): 395-402.

[26] LASSOUED FERJANI H, MAKHLOUF Y, MAATALLAH K, et al. Management of chronic recurrent multifocal osteomyelitis: review and update on the treatment protocol [J]. Expert opinion on biological therapy, 2022, 22(6): 781-7.

[27] COBB L H, MCCABE E M, PRIDDY L B. Therapeutics and delivery vehicles for local treatment of osteomyelitis [J]. Journal of orthopaedic research : official publication of the Orthopaedic Research Society, 2020, 38(10): 2091-103.

[28] NURUZZAMAN F, ZHAO Y, FERGUSON P J. Chronic Nonbacterial Osteomyelitis: Insights into Pathogenesis, Assessment, and Treatment [J]. Rheumatic diseases clinics of North America, 2021, 47(4): 691-705.

[29] FANTONI M, TACCARI F, GIOVANNENZE F. Systemic antibiotic treatment of chronic osteomyelitis in adults [J]. European review for medical and pharmacological sciences, 2019, 23(2 Suppl): 258-70.

[30] LAWAL O U, BARATA M, FRAQUEZA M J, et al. Staphylococcus saprophyticus From Clinical and Environmental Origins Have Distinct Biofilm Composition [J]. Frontiers in microbiology, 2021, 12: 663768.

[31] SHARMA-KUINKEL B K, TKACZYK C, BONNELL J, et al. Associations of pathogen-specific and host-specific characteristics with disease outcome in patients with Staphylococcus aureus bacteremic pneumonia [J]. Clinical & translational immunology, 2019, 8(7): e01070.

[32] SAHOO A, SWAIN S S, PANDA S K, et al. In Silico Identification of Potential Insect Peptides against Biofilm-Producing Staphylococcus aureus [J]. Chemistry & biodiversity, 2022, 19(10): e202200494.

[33] YANG D, ZHENG X, JIANG L, et al. Functional Mapping of Phenotypic Plasticity of Staphylococcus aureus Under Vancomycin Pressure [J]. Frontiers in microbiology, 2021, 12: 696730.

[34] DE FRUTOS F, OCHOA J P, NAVARRO-PEñALVER M, et al. Natural History of MYH7-Related Dilated Cardiomyopathy [J]. Journal of the American College of Cardiology, 2022, 80(15): 1447-61.

[35] !!! INVALID CITATION !!! .

[36] PARK J, PACKARD E A, LEVIN M G, et al. A genome-first approach to rare variants in hypertrophic cardiomyopathy genes MYBPC3 and MYH7 in a medical biobank [J]. Human molecular genetics, 2022, 31(5): 827-37.

[37] ROSE J, KRAFT T, BRENNER B, et al. Hypertrophic cardiomyopathy MYH7 mutation R723G alters mRNA secondary structure [J]. Physiological genomics, 2020, 52(1): 15-9.

[38] LOWEY S, BRETTON V, JOEL P B, et al. Hypertrophic cardiomyopathy R403Q mutation in rabbit β-myosin reduces contractile function at the molecular and myofibrillar levels [J]. Proceedings of the National Academy of Sciences of the United States of America, 2018, 115(44): 11238-43.

[39] YOUSAF M, KHAN W A, SHAHZAD K, et al. Genetic Association of Beta-Myosin Heavy-Chain Gene (MYH7) with Cardiac Dysfunction [J]. Genes, 2022, 13(9).

Figure legend

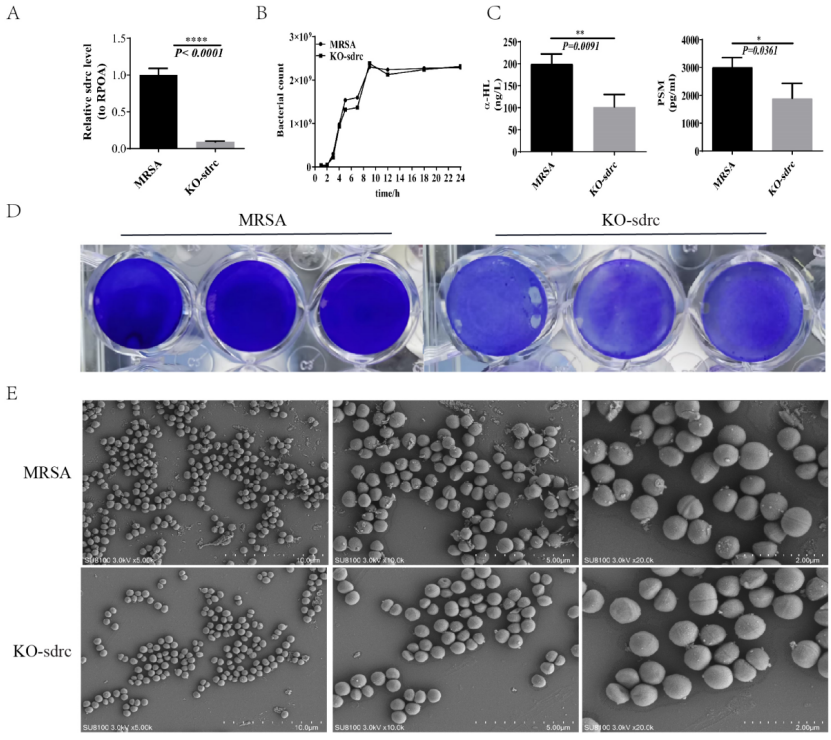

Figure 1: The effect of sdrc knockout on the formation of MRSA biofilm. A: RT-PCR was used to detect the knockout efficiency of sdrc, with rpoA as the internal reference. B: CCK8 detection of the impact of sdrc knockout on the growth ability of MRSA. C: ELISA detection of MRSA virulence pathogenic factors α-

Expression of HL and PSM. D: Crystal violet staining was used to observe the formation of MRSA biofilm. E: Scanning electron microscopy was used to observe the changes in surface morphology of MRSA.

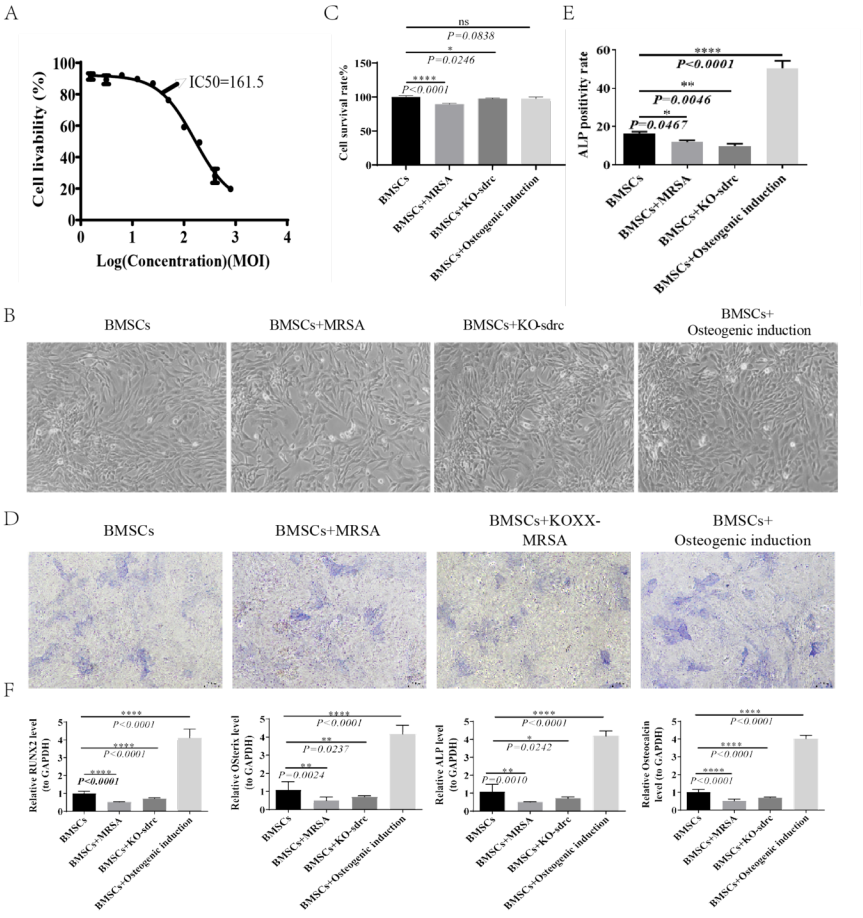

Figure 2: Effect of sdrc knockout on MRSA inhibition of BMSCs differentiation into osteoblasts. A: CCK8 detected the median lethal rate of MRSA on BMSCs cells (moi=number of MRSA/BMSCs). B: BMSCs cell culture (100X), by adding osteogenic inducers (100 mmol/L dexamethasone, 0.05 mmol · L-1 ascorbic acid, and 10 mmol · L-1) to BMSCs cells β- Sodium glycerophosphate for osteogenic differentiation induction. C: CCK8 was used to detect the proliferation activity of BMSCs cells. D: ALP staining (100X). E: Analysis of ALP staining positive rate. F: RT-PCR was used to detect the mRNA expression levels of osteogenic differentiation specific markers Runx2, Osterix (OSX), ALP, and Osteocalcin, using GAPDH as an internal reference.

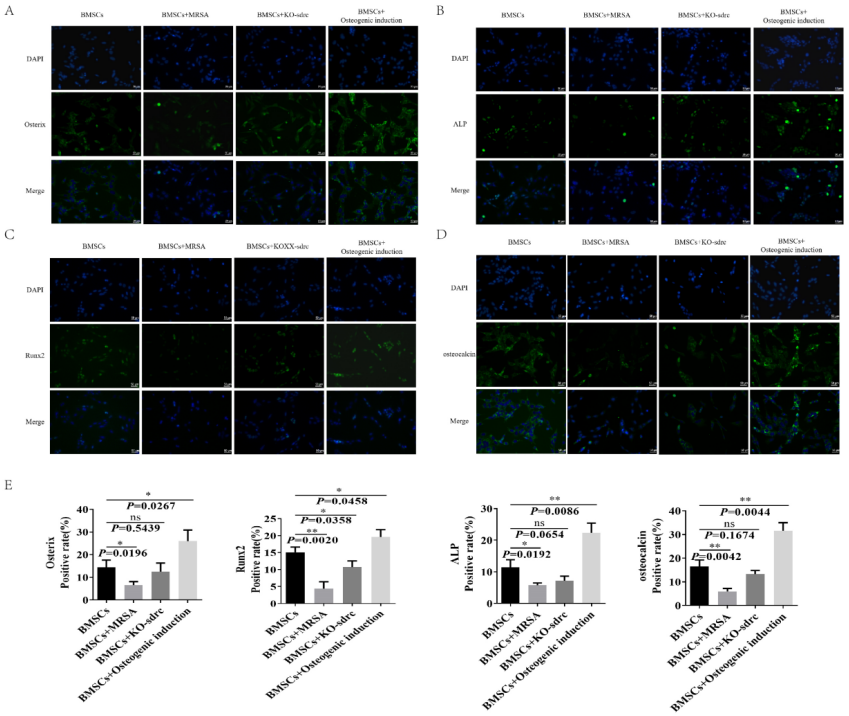

Figure 3: The IF experiment detected the expression of Runx2, OSX, ALP, and osteocalcin. A: OSX fluorescence map (200X). B: ALP fluorescence map (200X). C: Runx2 fluorescence image (200X). D: Osteocalcin fluorescence map (200X). E: Statistical chart of positive rates for Runx2, OSX, ALP, and Osteocalcin.

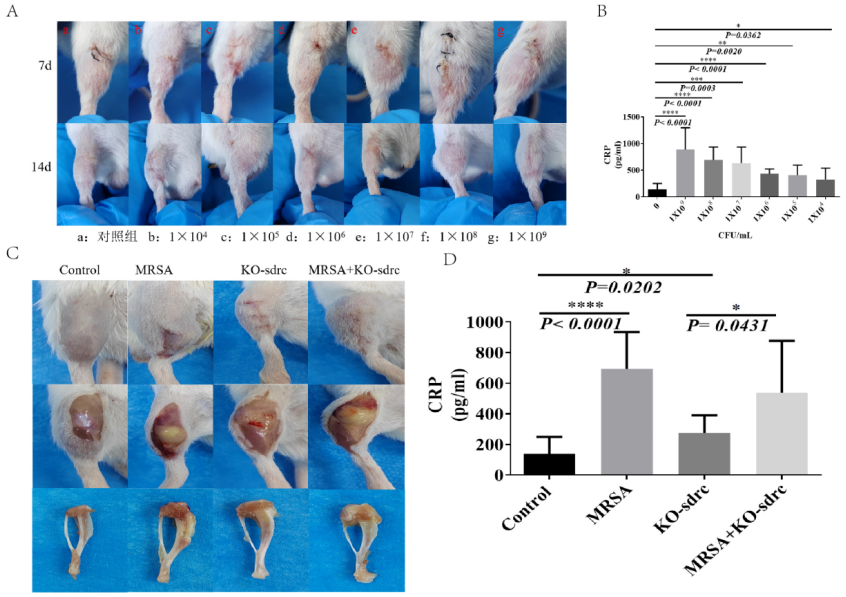

Figure 4: Selection of optimal MRSA infection concentration and construction of osteomyelitis model. A: Inject 1 separately $\times$ 10^4, 1 $\times$ 10^5, 1 $\times$ 10^6, 1 $\times$ 10^7, 1 $\times$ 10^8 and 1 $\times$ 10^9 CFU/mL MRSA was used to

construct an osteomyelitis model. B: ELISA detection of serum C-reactive protein content. C: Construct osteomyelitis models with optimal concentrations of MRSA, KO sdrc, and MRSA+KO sdrc. D: ELISA detection of serum C-reactive protein content.

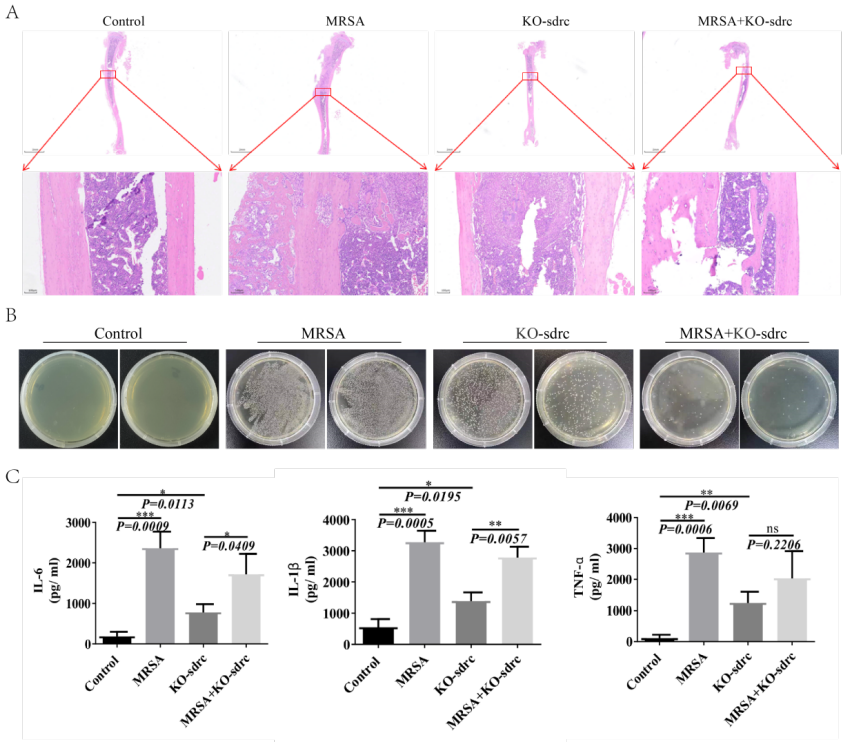

Figure 5: The effect of knocking out sdrc on the progression of osteomyelitis. A: HE staining was used to observe pathological changes (100X). B: Changes in bacterial content in wound exudate. C: ELISA detects the content of inflammatory factors.

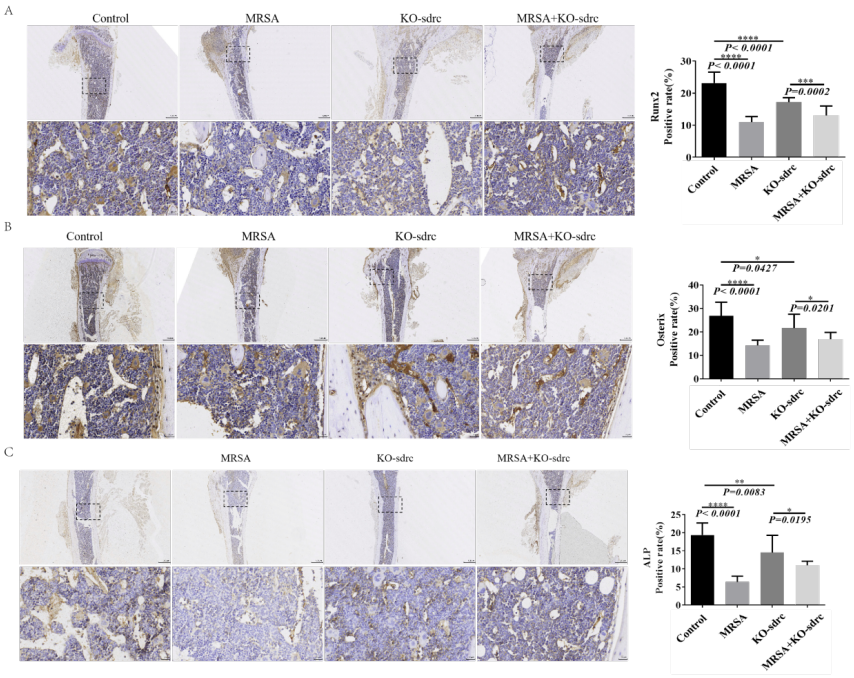

Figure 6. The effect of knocking out sdrc on MRSA inhibiting bone formation. A: IHC detected the expression of Runx2 (400X). B: IHC detected the expression of Osterix (400X). C: IHC detected the expression of ALP (400X).

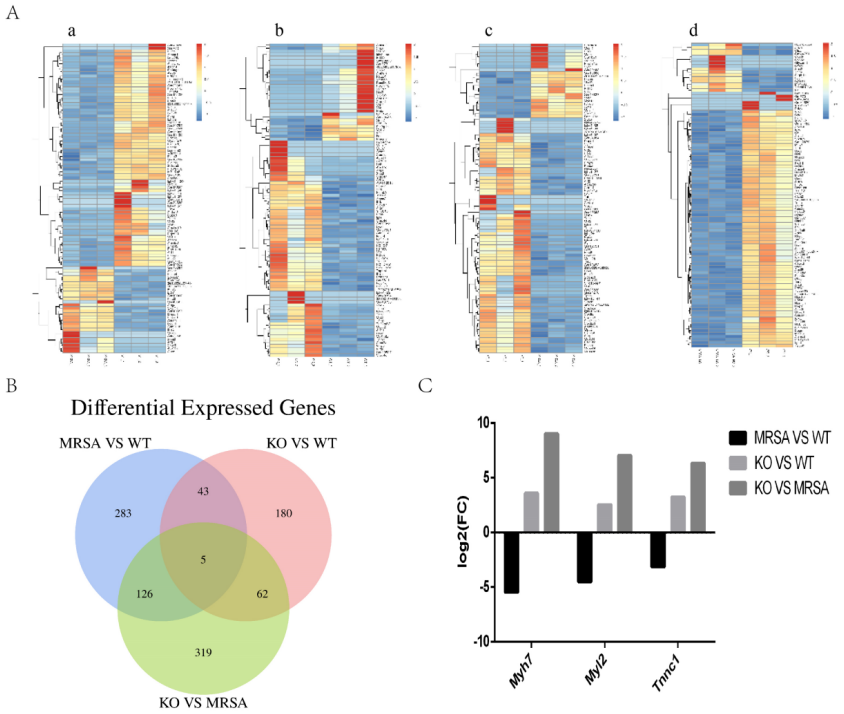

Figure 7 Transcriptome sequencing reveals the mechanism by which knocking out sdrc alleviates the progression of osteomyelitis. A: Differential gene expression clustering heatmap, a is MRSA VS WT; B is KO sdrc VS WT; C is KO sdrc VS MRSA; D is KO sdrc+MRSA VS WT.

B: Differential gene Wayne map. C: Differential gene expression multiple plot.

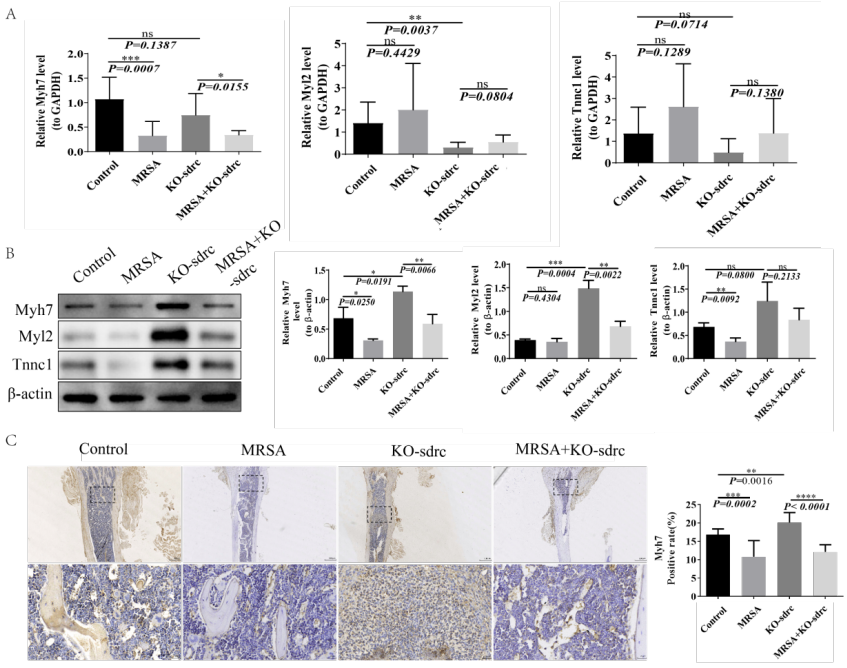

Figure 8 Transcriptome sequencing validation. A: RT-PCR was used to detect the expression of Myh7, Myl2, and Tnnc1, with GAPDH as the internal reference. B: WB detection of the expression of Myh7, Myl2, and Tnnc1, in order to β- Action as an internal parameter. C: IHC detected the expression of Myh7 (400X).

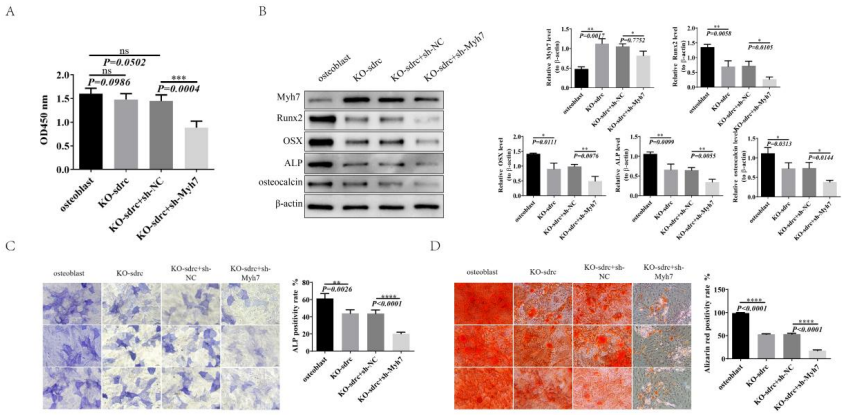

Figure 9: Knocking out sdrc promotes bone formation by promoting Myh7 expression. A: CCK8 was used to detect cell proliferation activity. B: WB detection of the expression levels of Myh7, Runx2, OSX, ALP, and osteocalcin, in order to β- Action as an internal parameter. C: ALP staining (100X). D: Alizarin red staining (100X).

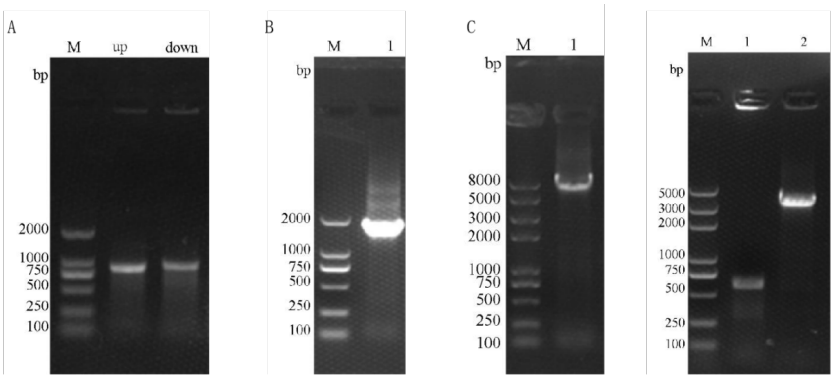

Figure Attachment 1 A: PCR validation of sdrC amplification fragment, with A and B fragments as templates, overlapping PCR amplification was performed to fuse AB fragments. B: Amplification of sdrC homologous arm fragments. C: 1% agarose gel electrophoresis amplification map was amplified by pKOR1 vector framework. D: The electrophoresis results of sdrC-JD-F/JD-R wild bacteria and knockout bacteria showed that 1 refers to the amplification product of knockout strain RN4220 $^{s}drc, and 2 refers to the control of wild bacteria RN4220$.

Figure Attachment 2: Construction of a stable osteoclast transfection strain interfered by Myh7. A: WB screening for the best interfering vector to β- Actin is an internal reference protein. B: RT-PCR validation of the optimal interference sequence, using GAPDH as the internal reference. C: The lentivirus was transfected into 293T cells for packaging (100X). D: Chronic virus infection of osteoclasts (100X).

Hosted file

`Tables.docx` available at https://authorea.com/users/760918/articles/736813-myh7-regulates-sdrc-protein-and-biofilm-formation-to-alleviate-osteomyelitis-induced-by-staphylococcus-aureus

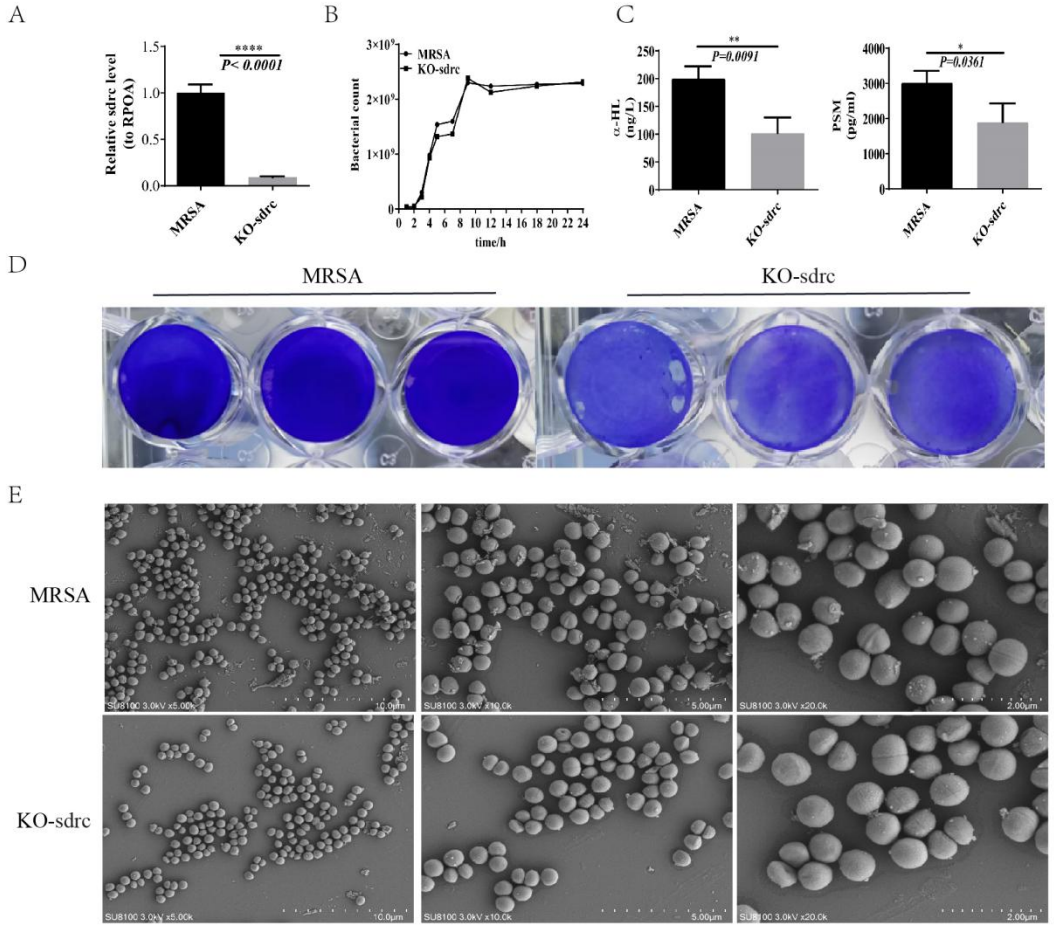
A
B
C
D
E
Relative sdrc level (to RPOA)
****
P< 0.0001
MRSA
KO-sdrc
Bacterial count
time/h
α-HL (ng/L)
**
P=0.0091
PSM (pg/ml)
*
P=0.0361
MRSA
KO-sdrc

Fig 1

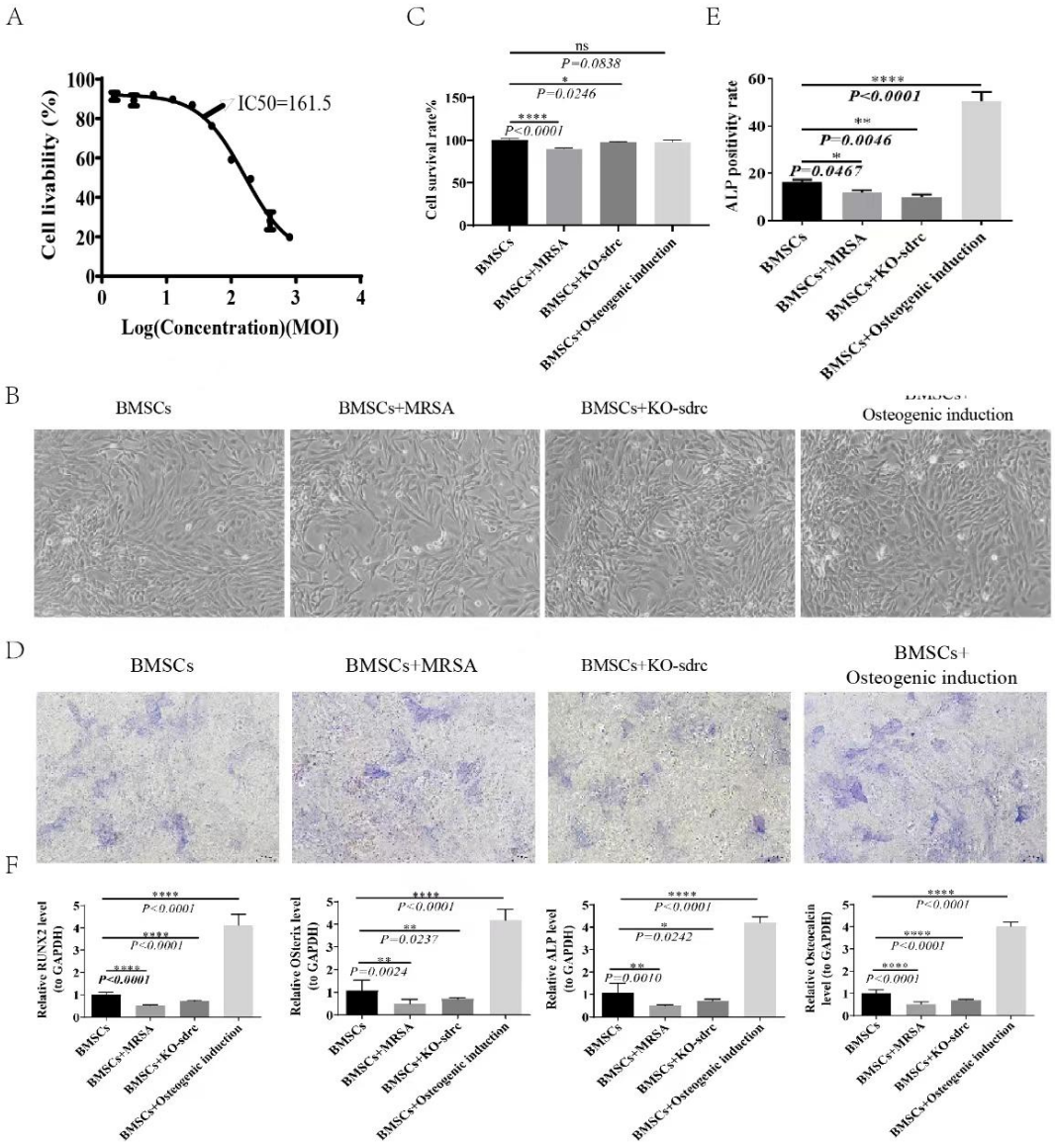
A
Cell livability (%)
IC50=161.5
Log(Concentration)(MOI)
C
Cell survival rate%
ns
P=0.0838
P=0.0246
P<0.0001
BMSCs
BMSCs+MRSA
BMSCs+KO-sdrc
BMSCs+Osteogenic induction
E
ALP positivity rate
P<0.0001
P=0.0046
P=0.0467
B
BMSCs
BMSCs+MRSA
BMSCs+KO-sdrc
Osteogenic induction
D
BMSCs
BMSCs+MRSA
BMSCs+KO-sdrc
BMSCs+
Osteogenic induction
F
Relative RUNX2 level (to GAPDH)
P<0.0001
Relative OSterix level (to GAPDH)
P=0.0024
P=0.0237
Relative ALP level (to GAPDH)
P=0.0010
P=0.0242
Relative Osteocalcin level (to GAPDH)

Fig 2

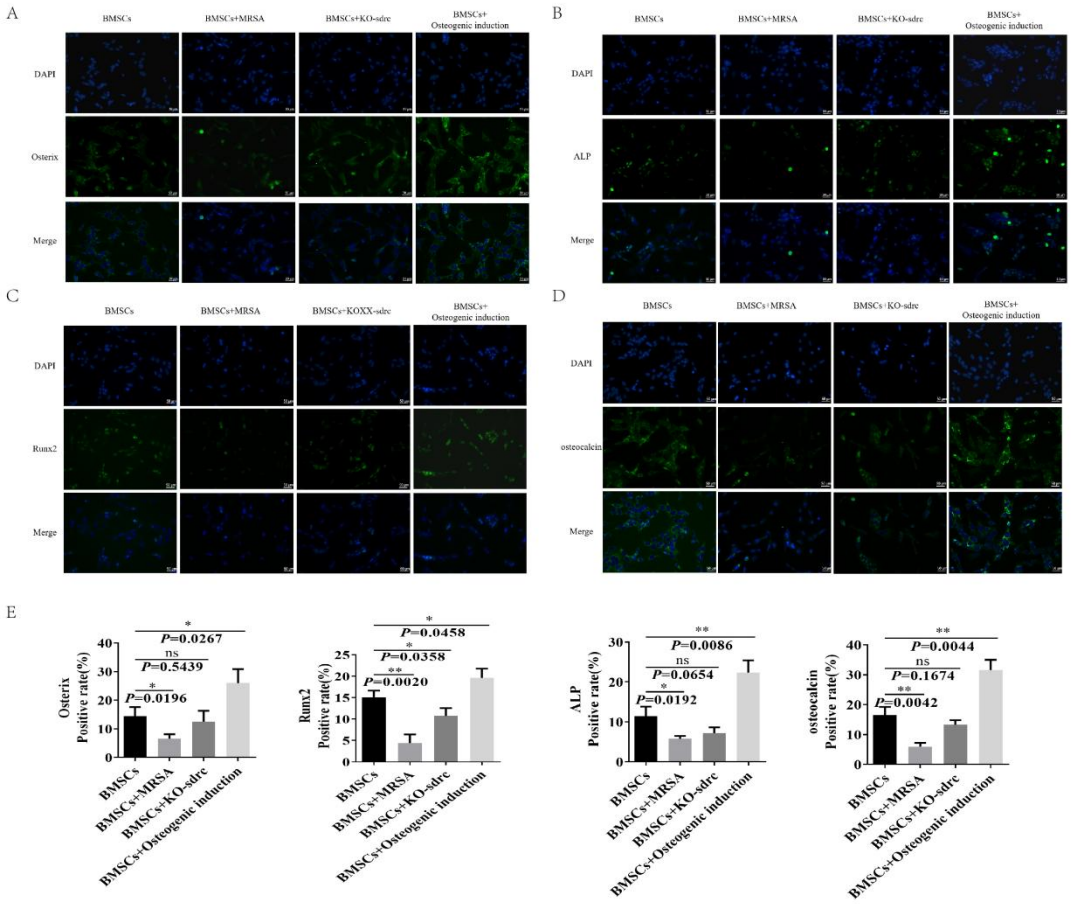
A
BMSCs
BMSCs+MRSA
BMSCs+KO-sdrc
BMSCs+ Osteogenic induction
DAPI
Osterix
Merge
B
ALP
C
BMSCs+KOXX-sdrc
Runx2
D
osteocalcin
E
Osterix Positive rate(%)
P=0.0267
P=0.5439
P=0.0196
Runx2 Positive rate(%)
P=0.0458
P=0.0358
P=0.0020
ALP Positive rate(%)
P=0.0086
P=0.0654
P=0.0192
osteocalcin Positive rate(%)
P=0.0044
P=0.1674
P=0.0042

Fig 3

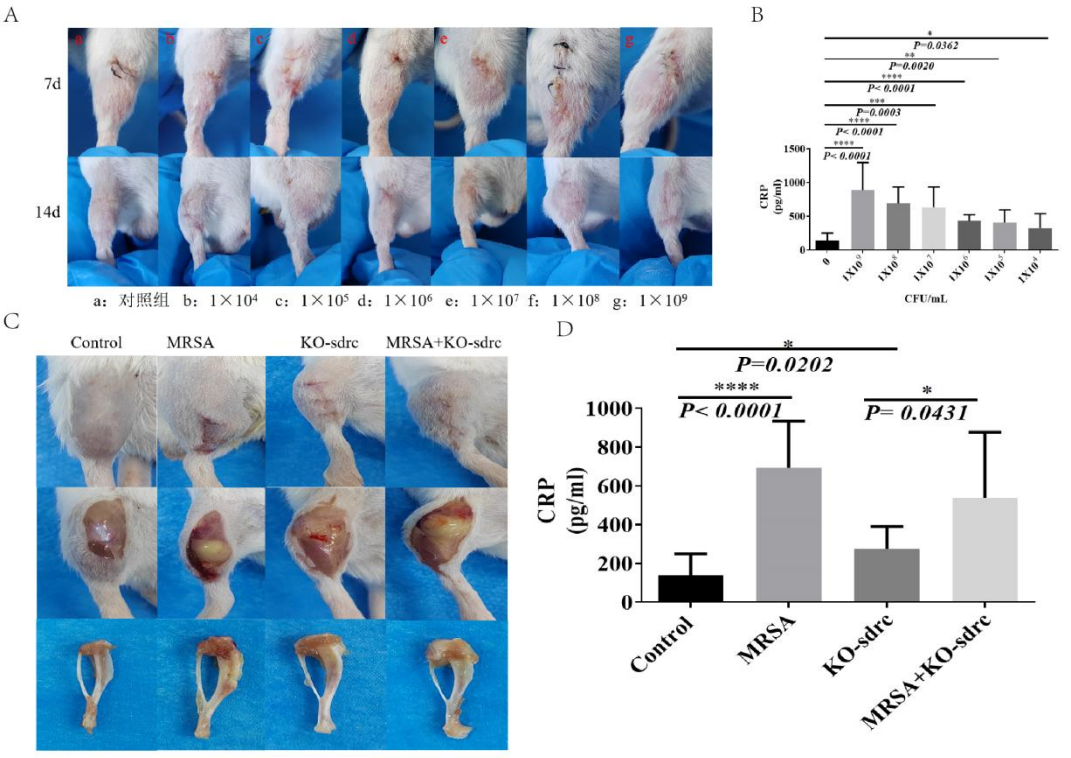
A
7d
14d
a: 对照组 b: 1×10⁴ c: 1×10⁵ d: 1×10⁶ e: 1×10⁷ f: 1×10⁸ g: 1×10⁹
B
P=0.0362
P=0.0020
P< 0.0001
P=0.0003
P< 0.0001
P< 0.0001
CRP (pg/ml)
CFU/mL
C
Control
MRSA
KO-sdrc
MRSA+KO-sdrc
D
P=0.0202
P< 0.0001
P= 0.0431
CRP (pg/ml)

Fig 4

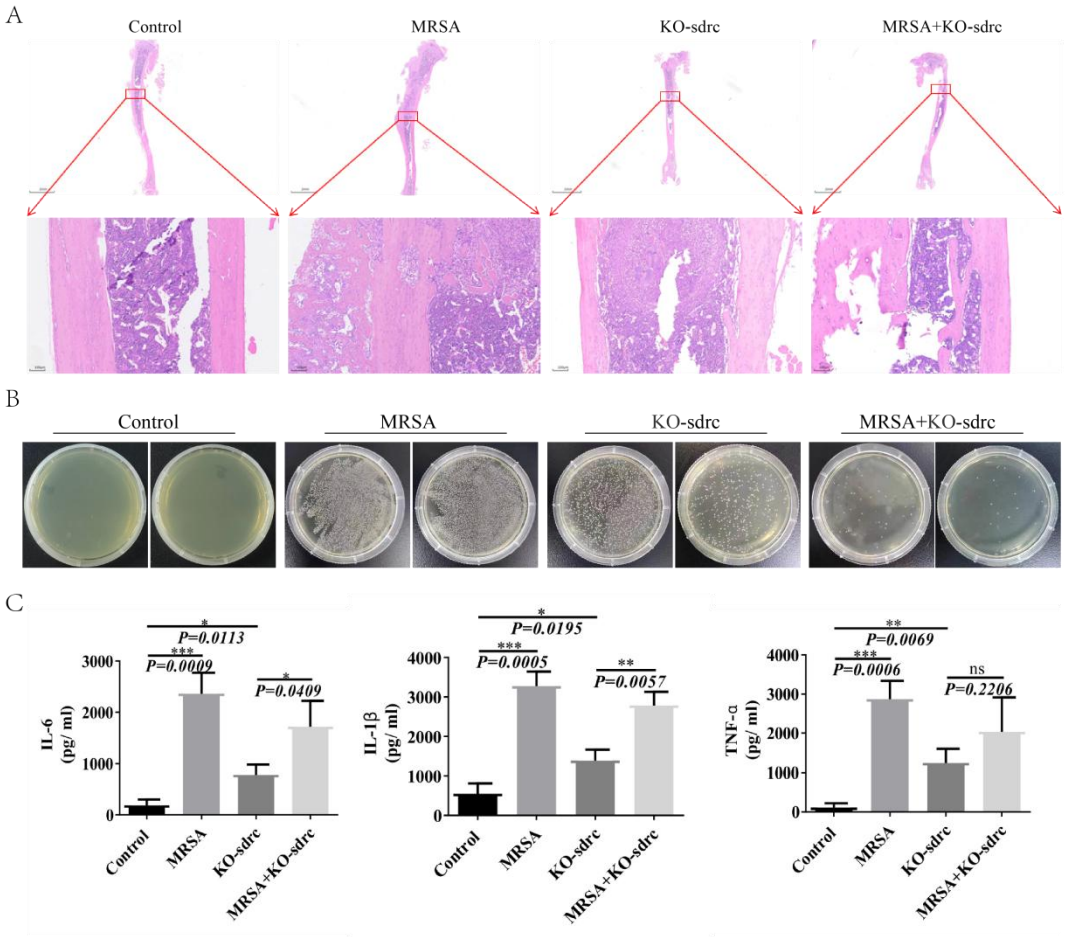
A
Control
MRSA
KO-sdrc
MRSA+KO-sdrc
B
Control
MRSA
KO-sdrc
MRSA+KO-sdrc
C
IL-6 (pg/ml)
P=0.0113
P=0.0009
P=0.0409
IL-1β (pg/ml)
P=0.0195
P=0.0005
P=0.0057
TNF-α (pg/ml)
P=0.0069
P=0.0006
ns
P=0.2206
Control
MRSA
KO-sdrc
MRSA+KO-sdrc

Fig 5

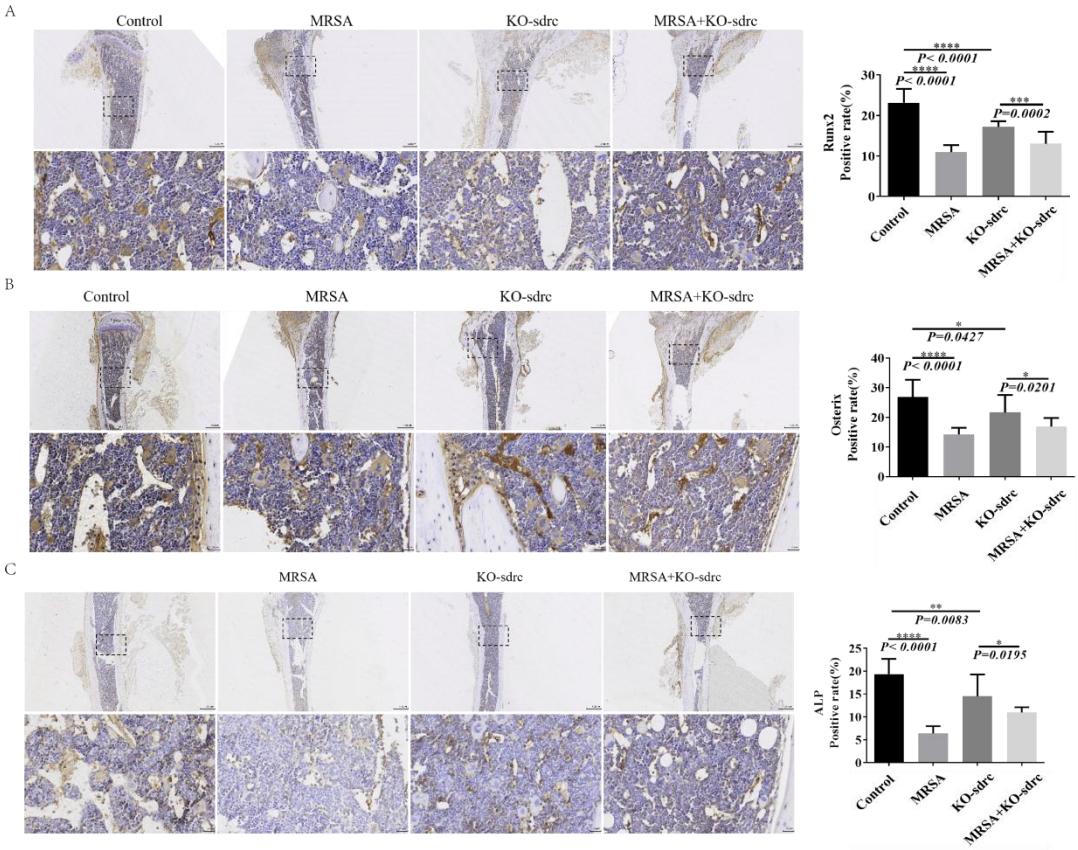
A
Control
MRSA
KO-sdrc
MRSA+KO-sdrc
Runx2
Positive rate(%)
P< 0.0001
P< 0.0001
P=0.0002
Control
MRSA
KO-sdrc
MRSA+KO-sdrc
B
Control
MRSA
KO-sdrc
MRSA+KO-sdrc
Osterix
Positive rate(%)
P=0.0427
P< 0.0001
P=0.0201
Control
MRSA
KO-sdrc
MRSA+KO-sdrc
C
MRSA
KO-sdrc
MRSA+KO-sdrc
ALP
Positive rate(%)
P=0.0083
P< 0.0001
P=0.0195
Control
MRSA
KO-sdrc
MRSA+KO-sdrc

Fig 6

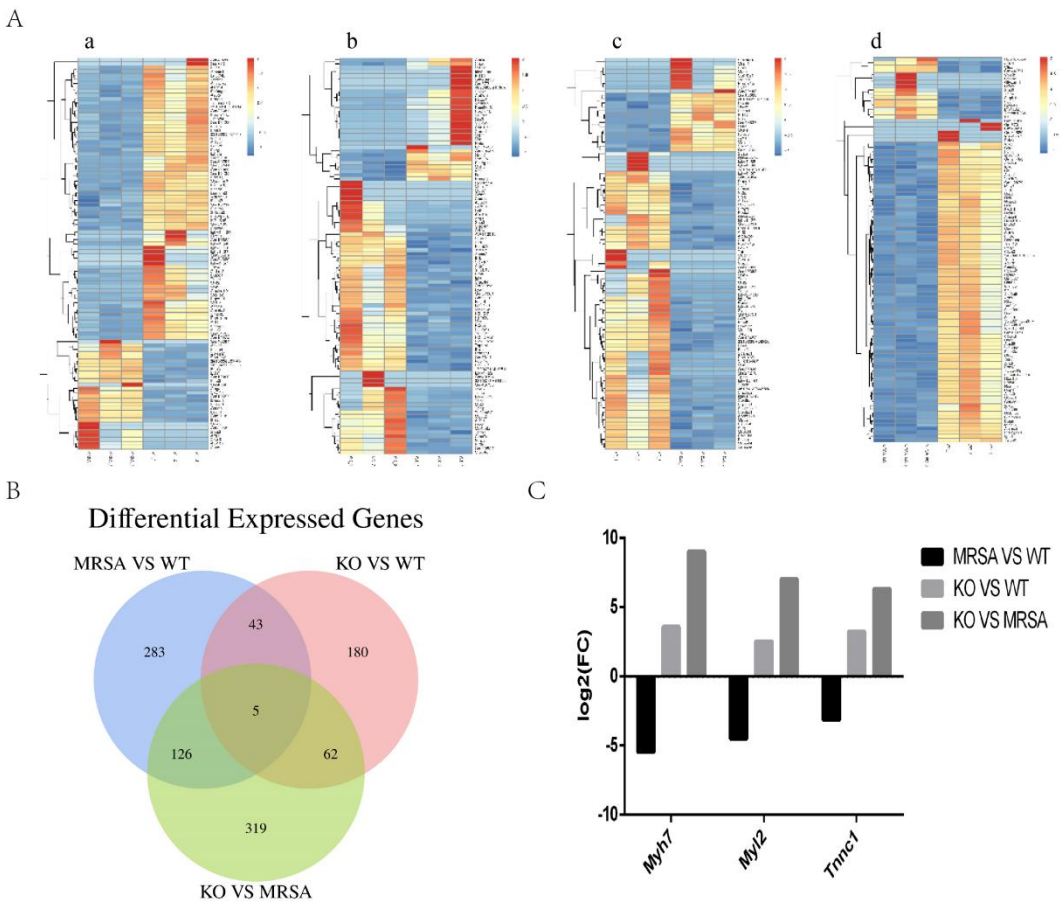
A
a
b
c
d
B
Differential Expressed Genes
MRSA VS WT
KO VS WT
KO VS MRSA
283
43
180
5
126
62
319
C
log2(FC)
10
5
0
-5
-10
Myh7
Myl2
Tnnc1
MRSA VS WT
KO VS WT
KO VS MRSA

Fig7

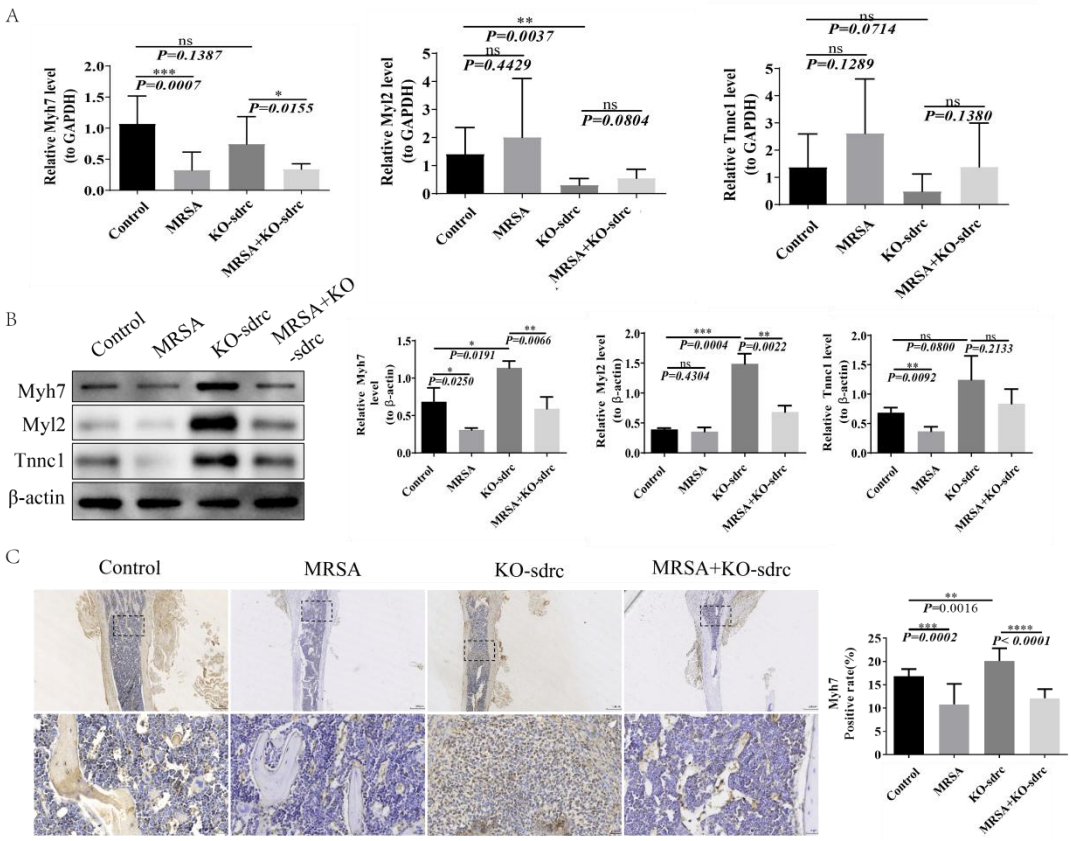
A
Relative Myh7 level (to GAPDH)
ns
P=0.1387
***
P=0.0007
*
P=0.0155
Relative Myl2 level (to GAPDH)
**
P=0.0037
ns
P=0.4429
ns
P=0.0804
Relative Tnnc1 level (to GAPDH)
ns
P=0.0714
ns
P=0.1289
ns
P=0.1380
Control
MRSA
KO-sdrc
MRSA+KO-sdrc
B
Control
MRSA
KO-sdrc
MRSA+KO-sdrc
Myh7
Myl2
Tnnc1
β-actin
Relative Myh7 level (to β-actin)
*
P=0.0191
**
P=0.0066
*
P=0.0250
Relative Myl2 level (to β-actin)
***
P=0.0004
**
P=0.0022
ns
P=0.4304
Relative Tnnc1 level (to β-actin)
ns
P=0.0800
ns
P=0.2133
**
P=0.0092
C
Control
MRSA
KO-sdrc
MRSA+KO-sdrc
Myh7 Positive rate(%)
**
P=0.0016
***
P=0.0002
****
P< 0.0001

Fig 8

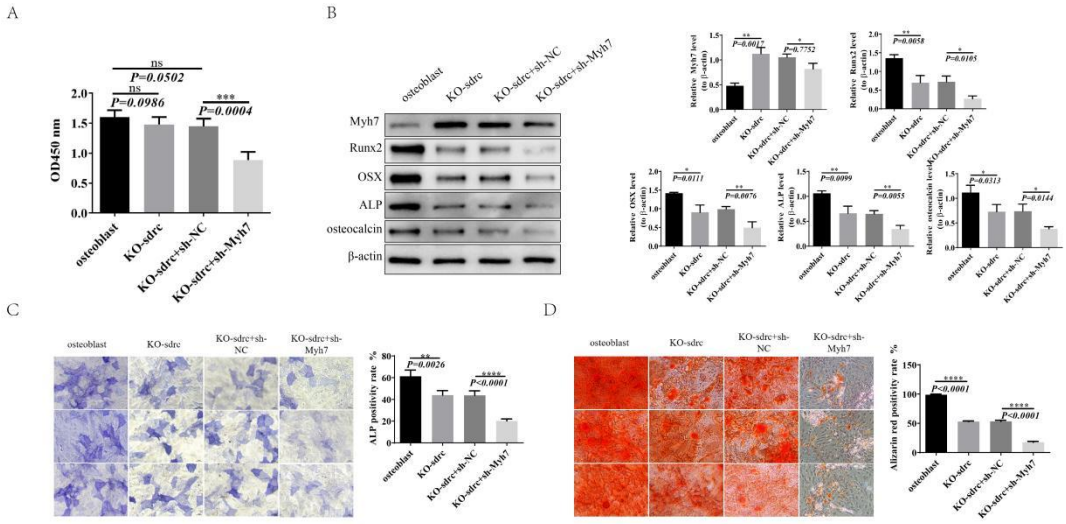
A
OD450 nm
ns
P=0.0502
ns
P=0.0986
***
P=0.0004
osteoblast
KO-sdrc
KO-sdrc+sh-NC
KO-sdrc+sh-Myh7
B
Myh7
Runx2
OSX
ALP
osteocalcin
β-actin
C
ALP positivity rate %
**
P=0.0026
****
P<0.0001
D
Alizarin red positivity rate %
****
P<0.0001
****
P<0.0001

Fig9